Simulation and Measurements of Small Arms Blast Wave Overpressure in the Process of Designing a Silencer

Nebojša Hristov[1], Aleksandar Kari[1], Damir Jerković[1], Slobodan Savić[2], Radoslav Sirovatka[3]

[1]Military academy, University of Defence, Pavla Jurisica Sturma, No.33, 11000, Belgrade, Serbia,
nebojsahristov@gmail.com, aleksandarkari@gmail.com, damir.d.jerkovic@gmail.com.
[2]Faculty of Engineering, University of Kragujevac, Sestre Janjic, No.6, 34000, Kragujevac, Serbia, ssavic@kg.ac.rs
[3]Military Technical Institute, Ratka Resanovića, No.1, 11000, Belgrade, Serbia, radesir@gmail.com

Simulation and measurements of muzzle blast overpressure and its physical manifestations are studied in this paper. The use of a silencer can have a great influence on the overpressure intensity. A silencer is regarded as an acoustic transducer and a waveguide. Wave equations for an acoustic dotted source of directed effect are used for physical interpretation of overpressure as an acoustic phenomenon. Decomposition approach has proven to be suitable to describe the formation of the output wave of the wave transducer. Electroacoustic analogies are used for simulations. A measurement chain was used to compare the simulation results with the experimental ones.

Keywords: Overpressure, silencer, decomposition approach, wave propagation, dotted wave source.

1. INTRODUCTION

PHENOMENA that occur when a gun is fired are the result of high powder gas energy that manifests through high intensity overpressure, high temperatures and high gas flow velocities. These phenomena can occur even at distances farther than 100 calibers from the muzzle. The flow-field around the muzzle of a gun barrel can be complicated and include flow phenomena such as expansion waves, compression waves, shocks, shear layers, and blast waves. The firing sound is a combination of a number of acoustic waves formed as a result of four main components: the gunpowder gas flow muzzle wave, the shock wave generated due to the supersonic projectile movement, the wave formed by the air column ejected from the gun barrel in front of the projectile and the acoustic wave generated by collision of gun parts during the firing process.

The main task of a silencer is to neutralize or reduce the first component of the firing sound without affecting the initial projectile velocity. The basic purpose of the silencer is to mask the position of the weapon, which can be precisely determined similarly to locating the blasting source [1]. A silencer suppresses the firing sound in several ways: by reducing the inner energy of the powder gases coming out of the barrel, by reducing their output velocity and temperature or by breaking the powder gas flow and by making it whirl.

The US Army's Ballistic Research Laboratory (BRL) has developed a prediction method for muzzle devices [2], based on gathered experimental data on muzzle devices for distances from 10 to 50 calibers from the muzzle [3, 4, 5]. The field distance from the muzzle, divided by a scaling length, is used as the universal independent variable to plot the peak overpressure. Free parameters are generated by the dimensional analysis and they are determined by the least squares fit to the data.

The resultant, which represents the free field muzzle blast, is computer simulated and can be applied on blast wave on surfaces in order to obtain the pressure.

It is well known that while the projectile accelerates with high temperature and high pressure, the explosion of propellant gases generates the muzzle blast wave [6, 7]. Since the muzzle energy increases, the impulsive wave intensity is estimated accordingly. A shot, as an impulse shock wave coming from the weapon, has a lot of negative effects on people and the environment. Unlike other sounds, shock wave has high energy, low frequency, impulsiveness, it is strongly directed and has long range propagation. [8]. Muzzle blast is strongly directed. The design of muzzle brake, which would decrease the noise, involves theoretic studies of acoustic systems and simulations as well as empirical and experimental data. [8].

The primary objective of this paper is to create a simulation model of a blast wave generated by small arms equipped with a silencer. The simulation model is based on electroacoustic analogies and application of decomposition approach. Measuring parameters on the experimental model yielded correct overpressure values at chosen characteristic points around the muzzle. The analysis of the obtained results has justified the use of the simulation model and its application in designing silencers for different types of small arms.

2. DESCRIPTION OF SILENCERS AS ACOUSTIC DEVICES

A silencer can be considered a gas-dynamic wave transducer inside which there are some connections and obstacles [9]. The wave transducer basically consists of the volume V_0 with connected acoustic transmitters (Fig.1.) that border on the volume V_0 with their cross-sections S_β ($\beta=1$, 2). The volume V_0 has energy connection with the environment only through acoustic transmitters in front of it and behind it. The cross sections S_1 and S_2 are called input cross-sections.
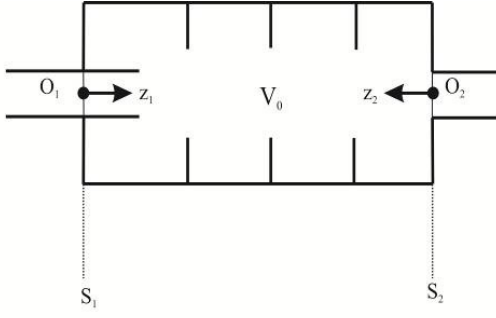
Fig.1. Formalization of an acoustic device.

The acoustic field of the wave transducer can be presented as superposition of translational and whirling waves [9]:

$$P_\beta(r,\alpha,z_\beta) = \sum_{k=1}^{\infty} c_{k(\beta)}^+ P_{k(\beta)}^+(r,\alpha,z_\beta) + c_{k(\beta)}^- P_{k(\beta)}^-(r,\alpha,z_\beta)$$
$$\vec{v}_\beta(r,\alpha,z_\beta) = \sum_{k=1}^{\infty} c_{k(\beta)}^+ \vec{v}_{k(\beta)}^+(r,\alpha,z_\beta) + c_{k(\beta)}^- \vec{v}_{k(\beta)}^-(r,\alpha,z_\beta) \tag{1}$$

where

β - the input cross-section index,

$c_{k(\beta)}^+$ - the amplitude of normal waves (decreasing),

$c_{k(\beta)}^-$ - the amplitude of reflected waves.

If (1) is applied, the acoustic field of the wave transducer has the following form, at the input cross-sections $S_\beta(\beta = 1,2)$:

$$P_\beta(r,\alpha,0) = \sum_{k=1}^{\infty} (c_{k(\beta)}^+ + c_{k(\beta)}^-) P_{k(\beta)}(r,\alpha)$$
$$\vec{v}_\beta^{\,t}(r,\alpha,0) = \sum_{k=1}^{\infty} (c_{k(\beta)}^+ + c_{k(\beta)}^-) \vec{v}_{k(\beta)}^{\,t}(r,\alpha) \tag{2}$$
$$\vec{v}_\beta^{\,z}(r,\alpha,0) = \sum_{k=1}^{\infty} (c_{k(\beta)}^+ - c_{k(\beta)}^-) \vec{v}_{k(\beta)}^{\,z}(r,\alpha)$$

The indices t and z stand for transversal and longitudinal components of the velocity vectors for the powder gas particles. Introducing:

$$a_{k(\beta)} = c_{k(\beta)}^+ + c_{k(\beta)}^-$$
$$b_{k(\beta)} = c_{k(\beta)}^+ - c_{k(\beta)}^- , \tag{3}$$
$$\beta = 1,2 \quad k = 1,2\ldots$$

the first and the third expressions in the system (2) take the following form:

$$P_\beta(r,\alpha,0) = \sum_{k=1}^{\infty} a_{k(\beta)} P_{k(\beta)}(r,\alpha)$$
$$\vec{v}_\beta^{\,z}(r,\alpha,0) = \sum_{k=1}^{\infty} b_{k(\beta)} \vec{v}_{k(\beta)}^{\,z}(r,\alpha) \tag{4}$$

The equation system (4) represents the solution of the boundary values for the Helmholtz equation under the condition that:

$$\int_{S_\beta} P_{k(\beta)}(r,\alpha)\vec{v}_{n(\beta)}^{\,z*}(r,\alpha)d\vec{S}_\beta = \delta_{kn} , \tag{5}$$

where:

$$d\vec{S}_\beta = \vec{z_0}dS_\beta,$$
$$\vec{v}_{n(\beta)}^{\,z*}(r,\alpha) = v_{n(\beta)}^{z*}(r,\alpha)\vec{z_0} , \qquad *\text{- complex value}$$
$$\delta_{\kappa n} = \begin{cases} 0,........k \neq n \\ 1,........k = n \end{cases}$$

Any acoustic field at the input cross-sections S_β of the wave transducer can be expanded to order (4). If all the input cross-sections of the wave transducer are expanded to order, then the coefficients of Fourier order are obtained $a_{k(\beta)}, b_{k(\beta)}$.

Integrating all the coefficients, we get the vectors:

$$a = (a_{1(1)}, a_{2(1)}, ..., a_{1(2)}, a_{2(2)}, ...),$$
$$b = (b_{1(1)}, b_{2(1)}, ..., b_{1(2)}, b_{2(2)}, ...). \tag{6}$$

If the environment inside the wave transducer is linear with no additional sources inside the transducer itself, the vectors a and b are mutually connected by

$$a = Zb \tag{7}$$

where Z has a matrix form. The matrix Z in the equation (8) represents the impedance matrix and it defines the relation between the pressure and the velocity. It is complex and can be expressed as:

$$Z^{\beta\gamma} = \begin{pmatrix} Z^{\beta\gamma}{}_{11} & Z^{\beta\gamma}{}_{12} & ... \\ Z^{\beta\gamma}{}_{21} & Z^{\beta\gamma}{}_{22} & ... \\ ... & ... & ... \end{pmatrix}, \beta,\gamma = 1,2. \tag{8}$$

where the $Z^{\beta\gamma}$ elements represent the infinite matrices.

At each cross-section of the wave transducer, the acoustic field can be shown in the form of superposition of normal and reflected waves by components $P_k(r,\alpha)$, $\vec{v}_k^{\,z}(r,\alpha)$ (1). The sum of all the coefficients $c_{k(\beta)}^+$, $c_{k(\beta)}^-$ (3) is given by the following vectors:

$$c^+ = (c_{1(1)}^+, c_{2(1)}^+, ..., c_{1(2)}^+, c_{2(2)}^+, ...)$$
$$c^- = (c_{1(1)}^-, c_{2(1)}^-, ..., c_{1(2)}^-, c_{2(2)}^-, ...) , \tag{9}$$

which are of the same type as the vectors a and b (1.7). Based on the equation (3), we get

$$a = c^+ + c^-, \ b = c^+ - c^- \quad (10)$$

The amplitudes of the normal and reflected waves in each cross-section are directly proportional through the scattering matrix R:

$$c^- = Rc^+ \quad (11)$$

The mutual relationship between the scattering matrix and the impedance matrix can be shown as:

$$Z = (I + R)(I - R)^{-1}, \ R = (Z + I)^{-1}(Z - I). \quad (12)$$

2.1. Decomposition approach to the description of wave processes during sound formation in the silencer

The area of the gas transducer between the input cross-sections S_1 and S_2 (Fig.2.) is divided by imaginary cross-sections into basic elements. The basic elements are regarded as acoustic wave transducers for which elements of the impedance matrix Z and the scattering matrix R are determined [9]. The elements of the scattering and impedance matrices of the wave transducer completely define the final recomposition results. Virtual lines, connected to the output cross-sections of the basic elements are considered to have infinitely small lengths during the recomposition. The recomposition of the basic elements into virtual conductors is performed in accordance with the conditions determined by the continuity of the pressure and the longitudinal component of the gas particle velocity for two adjacent cross-sections connecting the basic elements. A multi-chamber silencer (Fig.2.) is used to demonstrate the decomposition approach.
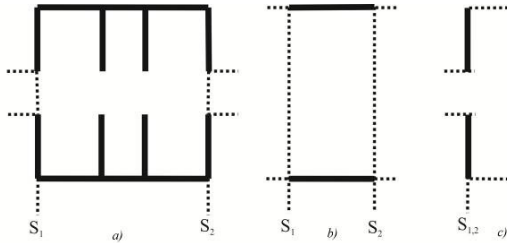

Fig.2. Basic elements of the wave line a - silencer, b- cutout of the cylindrical conductor, c-a membrane between two cylindrical cutouts.
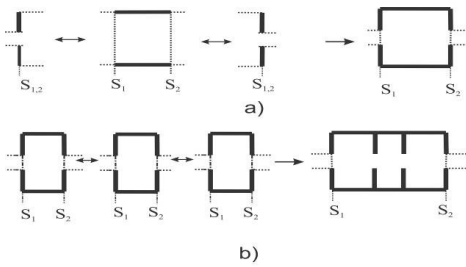

Fig.3. Recomposition of the basic elements: a – a chamber consisting of connectors and a cylindrical line; b –a multi-chamber silencer obtained by joining chambers.

In order to set a mathematical model of the multi-chamber silencer, a cutout of the cylindrical wave conductor (Fig.2.b)) and membranes of two cylindrical lines of different diameters (Fig.2.c)) are used as basic elements.

If two membranes and one cylindrical line cutout are joined, a silencer chamber is obtained (Fig.3.a)). Joining three chambers (Fig.3.b)) yields a multi-chamber silencer.

In Fig.2. and Fig.3., virtual conductors are presented by dashed lines. The membrane of the two cylindrical lines of different diameters has no volume, i.e., there is no impedance matrix. As to the elements of the scattering impedance matrices of the cylindrical cutouts and membranes, a method developed in electrical engineering is used [9, 10]. The scattering matrix of the cylindrical cutouts has the following structure:

$$R = R^{\alpha\alpha} - (R^{\alpha\beta} R^{\alpha\gamma}) \begin{pmatrix} -R^{\beta\beta} & I \\ I & -R^{\gamma\gamma} \end{pmatrix}^{-1} \begin{pmatrix} R^{\beta\alpha} \\ R^{\gamma\alpha} \end{pmatrix}$$

$$R = \begin{pmatrix} 0 & D \\ D & 0 \end{pmatrix} \quad (13)$$

where:

0 – the zero matrix,

D - the diagonal matrix with the elements $D_{kn} = \delta_{kn} \exp(iG_n l); k, n = 1, 2, ...,$

G_n - the coefficient of wave propagation in the conductor,

l - the length of the conductor cutout.

The impedance matrix of the cylindrical cutouts is:

$$Z = \begin{pmatrix} Z^{11} & Z^{12} \\ Z^{21} & Z^{22} \end{pmatrix} \quad (14)$$

where

$$Z_{kn}^{11} = Z_{kn}^{22} = -\delta_{kn} ctg G_n l;$$

$$Z_{kn}^{12} = Z_{kn}^{21} = -\delta_{kn} \cos ec G_n l;$$

The scattering matrix of the membranes between the conductors has the following structure:

$$R = \begin{pmatrix} A & -I \\ I & A^T \end{pmatrix}^{-1} \begin{pmatrix} -A & I \\ I & A^T \end{pmatrix}, \quad (15)$$

where A^T - transpositioned matrix A, whose elements are determined using the formula:

$$A_{kn} = \int_{S_2} P_{n(1)}(r, \alpha) \vec{v}_{k(2)}^{Z*}(r, \alpha) \cdot d\vec{S_2}, k = 1, 2, ... \quad (16)$$

2.2. Electroacoustic and electromechanical analogies

All the phenomena occurring during the firing of a weapon can be described as acoustic processes; hence, it is quite simple to register the acoustic pressure (powder gas overpressure) of the sound wave. The silencer can be considered an acoustic system with input values at the muzzle and output values at the point M (Fig.4.).
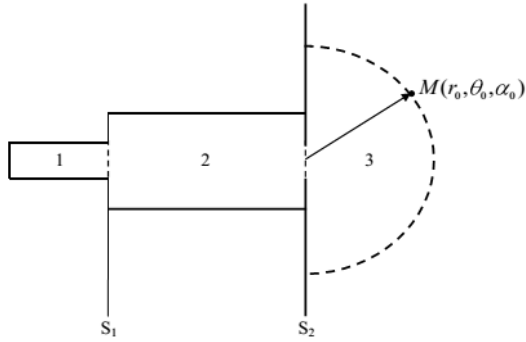

Fig.4. Scheme of overpressure measurement at the point M
S_1- muzzle cross-section, S_2- output cross-section of the silencer.

Fig.5. Equivalent acoustic a) and electrical system b).

Applying electroacoustic analogies [10], the acoustic sound suppressing device can be interpreted using an adequate oscillating electrical circuit decomposed into its constituting components (Fig.5.).

The volumes of the chambers (Fig.6.b), Fig.6.c) and Fig.6.d)) represent the acoustic capacitance that is obtained by

$$C_a = \frac{V}{\rho c^2} .$$ (17)

The chamber capacitance does not depend on its form but only on the volume [10].

The lines connecting the chambers (Fig.6.a)) have their own inductance, i.e., they represent the mass of the air column to be suppressed. The acoustic inductance is obtained using the expression [10]:
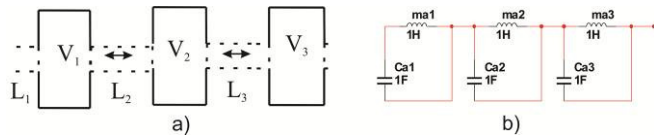
$$m_a = \frac{\rho l'}{S} ,$$ (18)

where l' is the adjusted length of the air column, i.e., the sum of the length of the line l and the adjusted length Δl in accordance with the connection diameter (Fig.6.a)). The length adjustment is performed according to the position of the connection in the acoustic system (Fig.6.b), Fig.6.c) and Fig.6.d)).

If the distances between the lines of the same cross-section are smaller compared to the adjustment of the cross-section, the air column is considered unique and its whole length is taken (Fig.6.e)).
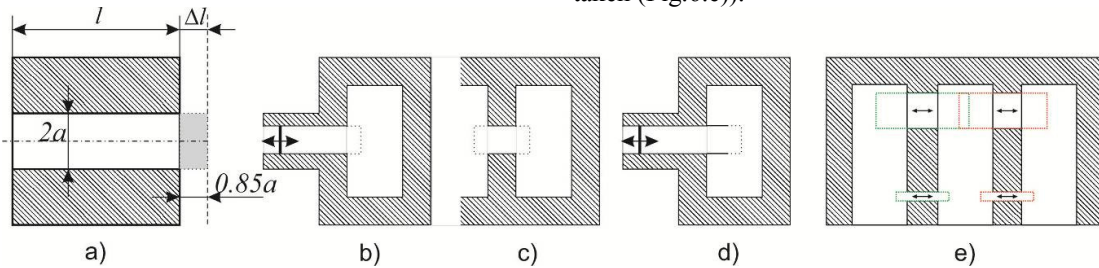

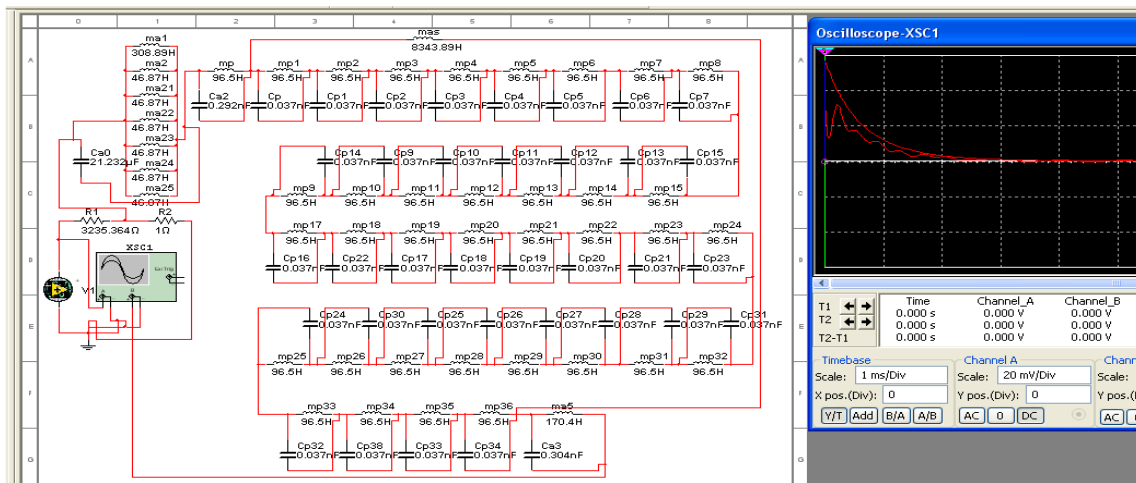Fig.6. Adjustment of the air column length of the acoustic inductance.

Fig.7. Simulation model of an electro-acoustic system.

3. SIMULATION OF PROCESSES IN ACOUSTIC DEVICES

Using the above stated analogies and applying the decomposition method, the silencer can be interpreted as an electrical oscillating circuit (Fig.7.).

The intensity of the powder gases pressure in the muzzle flow is introduced as an input parameter. The values are obtained by an internal ballistics calculation for a particular weapon.

The input signal is introduced by a signal-generator, and the output is recorded on a virtual oscilloscope. It is necessary to step the signal function for a time interval needed for the gas particles to travel from the sound way source (muzzle) to the referential point. The nature of the wave propagation after it has left the silencer [10] is identical to the wave propagation generated in an acoustic dotted source of the directed effect (Fig.8.).

The final signal values are obtained by applying the function of the distance from the referential point to the last opening on the silencer

$$p = \frac{1}{r}\sqrt{\frac{P_a \rho c}{4\pi}} \qquad (19)$$

and applying the propagation direction factor [10],

$$\Gamma_{(\vartheta)} = \frac{p_\vartheta}{p_0}. \qquad (20)$$

Simulations were performed for three cases: overpressure was measured around a weapon without a silencer, around the weapon equipped first with a silencer Type 1 and then with a silencer Type 2 (Fig.9.).

Silencer Type 1 (Fig.9.a)) is with an extended gunpowder gas flow. It consists of two expansion chambers, membrane for flow breaking and extended powder gas flow. The extended flow is formed within the cutout at 36 perforated membranes, which are turned at the angle of 10º, so that the whole flow is 2π. The silencer Type 2 (Fig.9.b)) has a simpler design. It consists of five expansion chambers mutually separated by a membrane for breaking the flow of gases and three flat membranes.

Simulation of overpressure is done at referential points in given directions and distances (Fig.10.).

In order to simplify the data processing, only maximum simulation values were taken from all the points.
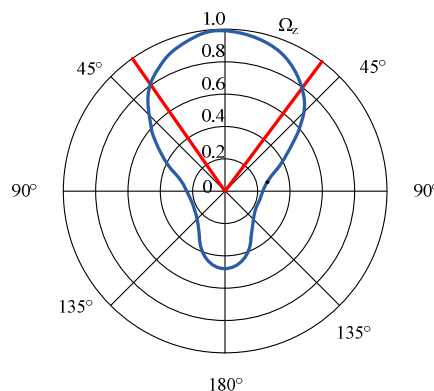

Fig.8. Propagation of the wave generated in an acoustic dotted source of directed effect.
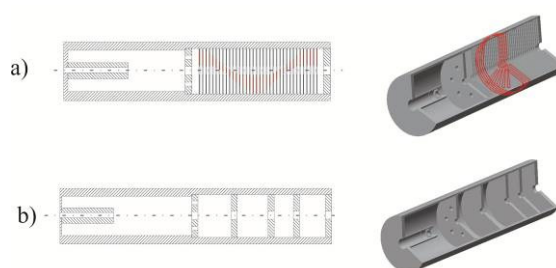

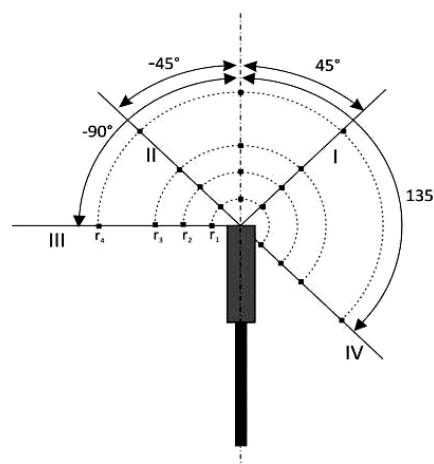Fig.9. Silencers (models in Creo) a) Type 1, b) Type 2.

Fig.10. Distribution of referential points (RP).

Table 1. Simulation values of the muzzle blast overpressure in bars.

	without a silencer				silencer Type 1				silencer Type 2			
	RP1	RP2	RP3	RP4	RP1	RP2	RP3	RP4	RP1	RP2	RP3	RP4
	-45°	45°	- 90°	135°	-45°	45°	-90°	135°	-45°	45°	-90°	135°
r												
0.2 m	0.46276	0.46276	0.22831	0.15214	0.0466	0.0466	0.0172	0.0138	0.0409	0.0409	0.0151	0.0121
0.4 m	0.23138	0.23138	0.11415	0.07607	0.0233	0.0233	0.0086	0.0069	0.0204	0.0204	0.0075	0.006
0.6 m	0.15428	0.15428	0.07611	0.05072	0.0154	0.0154	0.0057	0.0046	0.0136	0.0136	0.005	0.004
1.0 m	0.09255	0.09255	0.04566	0.03043	0.0104	0.0104	0.0038	0.0031	0.0092	0.0092	0.0034	0.0027

4. MEASUREMENT METHOD DESCRIPTION

Measuring overpressure in the time base provides not only the peak overpressure values but also some information on the nature of the blast wave. Measurement systems based on the principle of piezoelectric effect are most suitable for use here. Generated charge (based on the piezo-converter) is introduced into the intermediate unit - amplifier via coaxial cable and then into a special registration device. In order to obtain an entirely physical image of this impulse phenomenon, several providers are used as presented in the flow chart (Fig.11.).
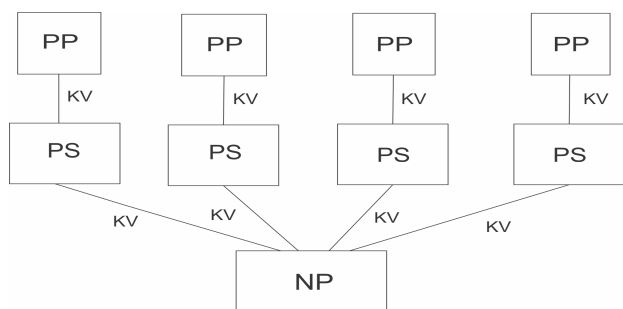

Fig.11. Flowchart for measurements and data collection.
PP pressure converter, PS - intermediate unit, KV - coaxial line, NP - data carrier.

Piezotronics probes PCB 137A23 (PP Fig.11.) were used to measure overpressure, while the charge amplifier 494A21 PCB piezotronics (PS Fig.11.) was used as an amplifying unit in the measurement system.

The muzzle blast overpressure was measured first without the use of a silencer and then, under the same conditions (atmospheric pressure 998 mbar, temperature 20°C), the overpressure was measured with the use of two types of silencers.

Since the same measurement chain was used, the measurement error has no effect on the obtained results.

The overpressure was measured at referential points (Fig.12.) in compliance with the scheme identical to the one used for simulation (Fig.10.).
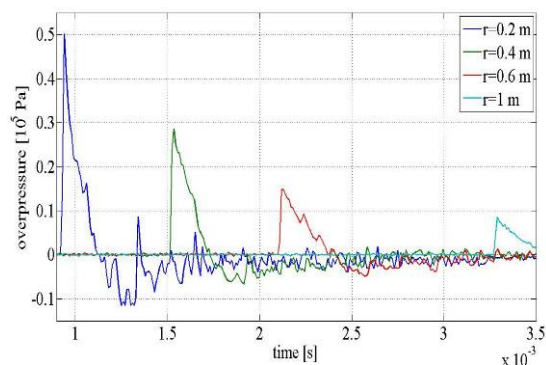
In addition to the overpressure intensity, the projectile velocity was measured [11, 12] in order to establish the effect of the silencer on the initial elements of the projectile flight towards the target.

Fig.12. Displaying of measurement methods.
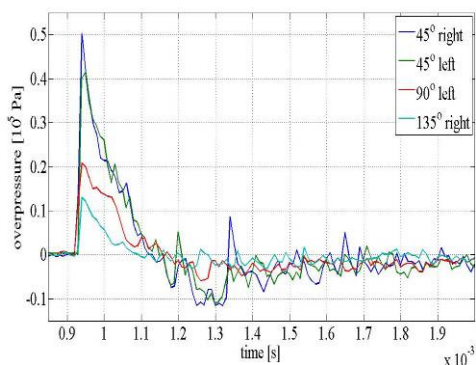
a) Measured overpressure for the same distance (r = 0.2 m) and different angles

b) Measured overpressure for one angle (45° right) and different distances

Fig.13. Overpressure measured using the probe PCB137A23 in the time domain (without a silencer).

Table 2. Values of the measured muzzle blast overpressures in bars.

	without a silencer				silencer Type 1				silencer Type 2			
	RP1	RP2	RP3	RP4	RP1	RP2	RP3	RP4	RP1	RP2	RP3	RP4
R	-45°	45°	-90°	135°	-45°	45°	-90°	135°	-45°	45°	-90°	135°
0.2 m	0.4513	0.4405	0.2111	0.1232	0.05388	0.03344	0.01074	0.009757	0.03657	0.04312	0.01365	0.009236
0.4 m	0.2767	0.2828	0.1284	0.0846	0.02522	0.02295	0.00756	0.006801	0.02578	0.02297	0.00834	0.00723
0.6 m	0.1465	0.1573	0.0758	0.0544	0.01978	0.01506	0.00739	0.00653	0.0194	0.01601	0.00704	0.00665
1.0 m	0.0774	0.0794	0.0436	0.0306	0.015502	0.0111	0.00581	0.005216	0.01393	0.0116	0.00635	0.00607

Since there was no decrease in the initial velocity, it can be concluded that the silencers had no effect on the elements of the projectile flight. LabView software was used to record measurement results for numerical and graphical processing (Fig.13.).

Only the highest measured overpressure values for each measurement (the first maximum values in Fig.13.) were used in the analysis of the measurement results.

The peak overpressure average values at the referential points are shown in Table 2.

The experimental research included 137 measurements performed using the mentioned equipment. At each referential point, the described parameters were measured for three cases: without a silencer, with the silencer Type 1 and with the silencer Type 2. The measurement consisted of 5 to 10 single tests under the same initial conditions at each referential point. Standard deviation of the maximal measured overpressure values was less than 1 %. Based on the maximum deviation of registered overpressure values and the form of the change, as shown in the Fig.13., it can be concluded that the measured results show typical image of the pressure at each point of measurement and reliably represent the occurrence of the shock wave overpressure around the muzzle.

5. ANALYSIS OF THE OBTAINED RESULTS

The diagrams in Fig.14. give both the simulation and experimental results for the maximum muzzle blast overpressure values measured first without the use of a silencer, and then with the use of two types of silencers for different angles depending on the distance.

Simulation curves are fitted curves of the data obtained by simulation and measurements for the chosen points, per a form function:

$$y = Ae^{-Bx} \qquad (21)$$

which corresponds to the theoretical function of the pressure change during the period of the subsequent powder gases effect. The given coefficients A and B are calculated for each single experiment using the software.

Based on the shown diagrams it can be concluded that a silencer as an acoustic device reduces the peak overpressure ten times. The simulation results obtained by application of the decomposition approach are in good agreement with the experimental results. The simulation results for the angles of -45° and 90° show the least error, which is important for the silencer use.

The noticed error for the angles of 45° and 135° is the result of not taking into account the projectile rotation and air whirling, which are negligible.

This paper gives a comparative analysis of the obtained results for the muzzle blast overpressure peak under given conditions and at given distances without the use a silencer and with the use of two types of silencers.

The average reduction level of overpressure for both types of silencer, for all observed directions and distances, is similar. For the silencer Type 1, the average reduction level of overpressure was 89.35 %, and for the silencer Type 2 it was 90.22 %. It was observed that with increasing the distance, the reduction level of the silencer Type 2 decreases (at the distance of 0.2 m the reduction level is about 92 %, while at the distance of 1 m it is about 87 %). With increasing the distance, the reduction level of the silencer Type 1 does not decrease significantly, thus showing better reduction characteristics at the longer distances.
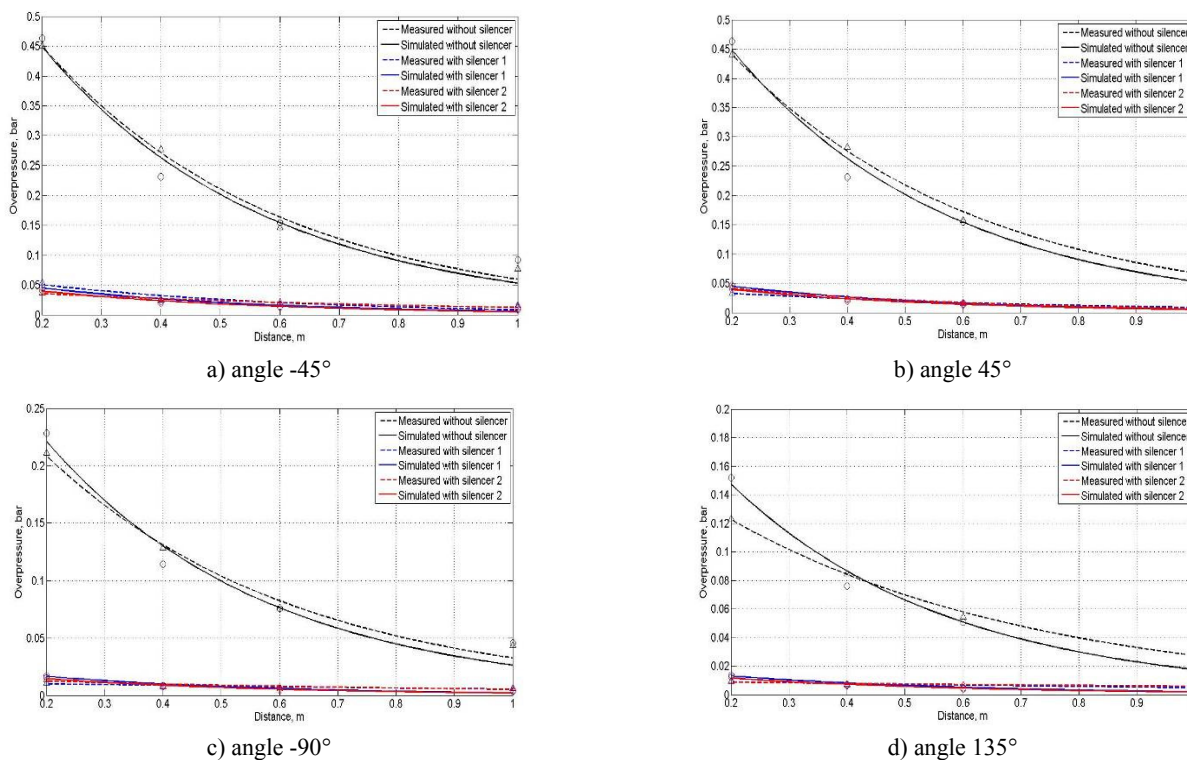

a) angle -45°

b) angle 45°

c) angle -90°

d) angle 135°

Fig.14. Diagrams of measurement and simulation results in the given directions.

6. Conclusions

The silencer with an extended (spiral) powder gas flow has been noticed to exhibit better performance in reducing muzzle blast overpressure at longer distances.

Due to the occurrence of noise and small values of overpressure, recording of data at larger distances is very difficult and it was not performed.

Decomposition approach and electroacoustic analogies were used to simulate the silencer performance.

The simulation results are in good agreement with the experimental results, which together with other advantages of simulation (cheap, fast, no need for experiments) justify its use.

Mean deviation of the simulated values of the maximum overpressure in the referential points, for all directions and distances, is less than 6.5 % (for directions it is about 2.8 %, and for distances it is about 7.8 %), compared to the mean maximum measured values. These deviations are average for all three cases (with and without silencers Type 1 and Type 2)

The simulation method offers many possibilities like a simple way to change distances and referential point angles, which practically means that the whole area around the silencer can be simulated. It is also very easy to generate the input signal for any kind of weapon, while the desired type of a silencer can be modeled using the right combination of its constituent elements. Time needed for preparation of a new simulation model is very short, and the simulation results are obtained quickly.

However, usefulness of this simulation model needs to be further evaluated in experimental tests for other calibers, especially for weapons with subsonic velocities of projectiles, followed by internal ballistic calculations.

After the model has successfully been used for other typical calibers of small arms, it could serve as a good basis for predictive design of silencers.

The simulation model is open to further improvement until it becomes fully automatized by relating construction data from the 3D silencer model and final output parameters, by expanding the range of the output parameters, as well as by taking into account the parameters from the environment.

Acknowledgement

References

[1] Meng, X., Wang, Z., Zhang, Z., Wang, F. (2013). A method for monitoring the underground mining position based on the blasting source location. *Measurement Science Review*, 13 (1), 45-49.

[2] Smith, F. (1974). A theoretical model of the blast from stationary and moving guns. In *First International Symposium on Ballistics*, 13-15 November 1974, Orlando, Florida.

[3] Fansler, K.S., Thompson, W.P., Carnahan, J.S., Patton, B.J. (1993). *A parametric investigation of muzzle blast*. AD-A270 535. Army Research Laboratory, ARL-TR-227.

[4] Fansler, K.S. (1985). Dependence of free field impulse on the decay time of energy efflux for a jet flow. In *The Shock and Vibration Bulletin*, Part 1. Washington, DC: The Shock and Vibration Center, Naval Research Laboratory, 203-212.

[5] Heaps, C.W., Fansler, K.S., Schmidt, E.M. (1985). Computer implementation of a muzzle blast prediction technique. In *The Shock and Vibration Bulletin*, Part 1. Washington, DC: The Shock and Vibration Center, Naval Research Laboratory, 213-230.

[6] Rehman, H., Hwang, S.H., Fajar, B. et all. (2011). Analysis and attenuation of impulsive sound pressure in large caliber weapon during muzzle blast. *Journal of Mechanical Science and Technology,* 25 (10), 2601-2606.

[7] Kang, K.J., Ko, S.H., Lee, D.S. (2008). A study on impulsive sound attenuation for a high-pressure blast flowfield. *Journal of Mechanical Science and Technology,* 22 (2008) 190-200.

[8] Guo, Z., Pan, Y., Zhang, H., Guo, B. (2013). Numerical simulation of muzzle blast overpressure in antiaircraft gun muzzle brake. *Journal of Information & Computational Science,* 10 (10), 3013-3019.

[9] Golovanov, O.A., Smogunov, V.V., Grachev, A.I. (2008). The mathematical modeling of wave's processes in acoustic equipments based on decomposition algorithm. *Penza University Review*, 4 (20), 92-101.

[10] Kurtovic, H.S. (1982). *Basis of Technical Acoustic* (in Serbian). Belgrade, Serbia: Naučna knjiga.

[11] Li, H., Lei, Z. (2013). Projectile two-dimensional coordinate measurement method based on optical fiber coding fire and its coordinate distribution probability. *Measurement Science Review,* 13 (1), 34-38.

[12] Zhao, Z., Wen, G., Zhang, Y., Li, D. (2012). Model-based estimation for pose, velocity of projectile from stereo linear array image. *Measurement Science Review,* 12 (3), 104-110.